

Detecting sound waves generated by leaks in buried water distribution pipes

Ray Kirby (1), Wenbo Duan (2), Mahmoud Karimi (3), Michael Brennan (4), and Nicole Kessissoglou (3)

(1) Centre for Audio, Acoustics and Vibration, University of Technology Sydney, Sydney, Australia

(2) Brunel Innovation Centre, Brunel University London, London, United Kingdom

(3) School of Mechanical and Manufacturing Engineering, University of New South Wales, Sydney, Australia

(4) Department of Mechanical Engineering, UNESP, São Paulo, Brazil

ABSTRACT

It is common to use guided sound waves to detect leaks or cracks in pipelines. Applications include the non-destructive testing of oil and gas pipelines, which normally takes place at ultrasonic frequencies, as well as the detection of leaks and ruptures in water filled pipes at much lower audio frequencies. However, if the pipe is buried then sound leaks out of the pipe into the surrounding medium and this lowers the acoustic energy travelling along the pipe wall. This has the potential to limit the applications of this technology, and so it is necessary to develop knowledge of the acoustic properties of the guided waves in order to optimise detection techniques. Accordingly, this work examines the properties of sound waves propagating in an infinitely long fluid-filled buried pipe, with application to leak detection at low audio frequencies. A parametric study is undertaken to examine the sensitivity of sound propagation to the properties of the internal liquid, pipe walls and of the surrounding medium.

1 INTRODUCTION

The use of sound waves to monitor the condition of structures such as pipelines is now very common. In the ultrasonic frequency range, elastic waves are guided down the walls of a pipe and they are used to detect cracks or regions of corrosion before they develop into ruptures. Alternatively, one may detect acoustic emissions generated by a leak or rupture in a pipe, and these are normally analysed in the low audio frequency range. This latter application is becoming increasingly important in the detection of leaks from water pipes, as the pipe networks begin to age. Accordingly, this article focusses on investigating the sensitivity of existing acoustic based detection techniques to those environmental conditions typically encountered when monitoring water-filled pipelines.

The leakage or rupture of a water-filled pipe acts as an acoustic source, which then excites a sound wave that travels down the pipeline. When one moves away from the acoustic near field of the source, the acoustic energy propagates in a series of discrete eigenmodes that are characteristic of the coupled water-pipe system. At low audio frequencies, three axisymmetric modes can propagate in a water-filled pipe (Muggleton 2013): (i) a coupled, compressional, fluid type mode, in which the majority of the acoustic energy lies in the fluid, this is called here the $s = 1$ mode; (ii) a coupled, compressional, structural type mode, in which the majority of the acoustic energy lies in the pipe wall, this is called here the $s = 2$ mode; and, (iii) an uncoupled shear, or torsional, mode in which the acoustic energy lies in the pipe wall only, and this is known as the $s = 0$ mode. These modes are defined in terms of their low frequency limit, where the acoustic energy in each mode is normally clearly located either in the fluid or the pipe wall; however, as one increases frequency then it is possible for the energy from, say, the $s = 1$ mode to transfer from the fluid to the wall, and vice versa for the $s = 2$ mode. Moreover, at higher frequencies the energy may move back and forth as the frequency changes, and many more coupled modes will propagate so that this problem becomes significantly more complicated (Nilsson 2008). Therefore, for leak detection it is convenient to operate in the low frequency range so that the behaviour of one or two eigenmodes is more readily understood.

It is, of course, common for pipelines carrying water to be buried underground, and this is known to further complicate the propagation of acoustic energy (Muggleton 2002). This is because the surrounding material couples to the pipe wall, and this supports the leakage of sound waves away from the wall in the form of compressional and shear waves (if the pipe is buried in a nominally solid material such as soil or sand). This leakage, or radiation, of acoustic energy is experienced as sound attenuation in the axial direction of the pipeline and this causes significant problems in ultrasonic applications where the amplitude of the guided wave can quickly become too small to detect (Leinov 2013, Duan 2016). However, at lower audio frequencies the axial attenuation imparted by the presence of surrounding material for the $s = 1$ mode is normally much lower, and so this mode can be used relatively successfully in the detection of leaks over relatively long lengths of pipe (Brennan 2017, Gao 2016). Moreover, the energy in the $s = 1$ mode is located primarily in the fluid and a number of commercial products take advantage of this by picking up the acoustic wave in the fluid rather than the pipe wall. The coupled nature of the

$s = 1$ mode also means that it is possible to detect this mode by placing sensors on the outside of the pipe wall. It is possible also to take advantage of the energy leaking from the pipe walls into the surrounding material and to try and detect compressional and shear waves travelling to the ground surface remote from the pipe location (Gao 2017). However, the radiation of acoustic waves from the pipe surface is complex and so it is necessary to build up an understanding of how the properties of the different elements of the coupled system affect the ability to develop a reliable detection methodology. Accordingly, this article investigates the influence of the material surrounding the pipe on the propagation of the $s = 1$ mode.

2 THEORY

The prediction of coupled acoustic wave propagation in fluid-filled buried pipelines presents a significant challenge, especially if one wishes to analyse all propagating eigenmodes over a wide frequency range. However, at lower audio frequencies, and for the detection of acoustics emissions, it is possible to simplify the problem and to focus only on the $s = 1$ mode. For example, many papers are now available that use approximate analytic techniques to find the properties of the $s = 1$ mode (Muggleton 2013, Gao 2016). Alternatively, Brennan et al. (Brennan 2017) show that numerical methods can also deliver good results, and they show good agreement between predictions obtained using the commercial software COMSOL and experimental measurements of the real part of the wavenumber and modal attenuation. However, parametric investigations tend to be easier to do using optimised computational methods and so the one-dimensional numerical approach described by Duan and Kirby (2016) is used here, as this is quick to use when finding coupled eigenmodes. This approach is based on the Semi Analytic Finite Element (SAFE) method and has the advantage of requiring only a one dimensional discretisation of the problem, and so this method is modified here to include the fluid in the pipe. This method involves expanding the pressure (p') and displacement fields (\mathbf{u}') as a sum over the system eigenmodes, so that

$$p'(r, \theta, z; t) = \sum_{m=0}^{\infty} \sum_{n=0}^{\infty} p_{m,n}(r) e^{i(\omega t - n\theta - \gamma_m z)} \quad (1)$$

$$\mathbf{u}'(r, \theta, z; t) = \sum_{m=0}^{\infty} \sum_{n=0}^{\infty} \mathbf{u}_{m,n}(r) e^{i(\omega t - n\theta - \gamma_m z)} \quad (2)$$

where r, θ, z form a cylindrical co-ordinate system, t is time, ω is the radian frequency, and $i = \sqrt{-1}$. In addition, for mode (m, n) , $p(r)$ and $\mathbf{u}(r)$ are the eigenvectors and γ is the coupled eigenvalue. In the analysis that follows, only axisymmetric modes are considered, so that $n = 0$. The modal expansions in Eqs. (1) and (2) are then substituted into the governing equations for the fluid and solid, which are given as

$$\nabla^2 p' - \frac{1}{c_0^2} \frac{\partial^2 p'}{\partial t^2} = 0 \quad (3)$$

$$(\lambda + \mu) \nabla(\nabla \cdot \mathbf{u}') + \mu \nabla^2 \mathbf{u}' = \rho \frac{\partial \mathbf{u}'}{\partial t^2} \quad (4)$$

where, c_0 is the speed of sound in the fluid, λ and μ are the Lamé constants, and ρ is density. Note that μ is also known as the shear modulus and henceforth this terminology will be used here. The modal expansions are then substituted into the governing equations and following the application of the appropriate boundary conditions an eigenproblem may be generated. At the internal diameter of the pipe, the appropriate boundary conditions are:

$$\frac{\partial p'}{\partial r} = \rho_0 \omega^2 u'_r, \quad p' = -\sigma'_{rr}, \text{ and } \sigma'_{\theta r} = \sigma'_{zr} = 0. \quad (5)$$

Here, ρ_0 is the density of the fluid, u_r is the pipe wall displacement in the r direction, and $\sigma'_{qi}(q, l = r, \theta \text{ or } z)$ is a symmetric stress tensor of rank two. To solve the problem the SAFE method is used, and this is carried out by using a weak form of the governing equations and applying a perfectly matched layer (PML) in the outer region where the surrounding material is placed. The PML is necessary because the SAFE method requires the outer domain to be closed, and at the exterior of this domain the following boundary conditions are applied:

$$\sigma'_{rr} = \sigma'_{\theta r} = \sigma'_{zr} = 0. \quad (6)$$

The boundary conditions at the outer perimeter of the PML are arbitrary, and so those in Eq. (6) are chosen because they are the most convenient for implementing the SAFE method. This technique is described in more detail by Duan and Kirby (2016). Solution of the eigenproblem is then implemented here using MATLAB, with a finite element mesh that uses three-noded quadratic line elements for each region, as well as an exponential

complex co-ordinate for the PML (Duan 2016). This yields an unordered list of eigenvalues and associated eigenvectors, which must then be sorted to separate radiation type modes from the leaky (axially propagating) modes, which are of interest in the current problem. This is accomplished by computing the kinetic energy density in each region, and then comparing the kinetic energy density in the PML with that in the fluid and pipe wall: those modes where the kinetic energy density in the fluid/pipe wall dominates are retained, all others are discarded. This is relatively straightforward for the $s = 1$ mode because the energy for this mode lies predominately in the fluid at low frequencies. Following the identification of the relevant eigenmodes(s), the phase speed, c , and attenuation, Δ , is then given as

$$c = \text{Re}(\omega/\gamma) \text{ and } \Delta = -20 \text{Im}(\gamma)/\ln(10). \quad (7a,b)$$

In addition, the energy located in the fluid and the pipe wall is also analyzed here in order to gain some understanding of how the system properties influence the distribution of energy within the system. Accordingly, the sound power in the fluid, W_0 , is given as

$$W_0 = \frac{\pi}{2\rho_0\omega} \int \text{Re}[p\gamma^*p^* + p^*\gamma p]rdr \quad (8)$$

and in the pipe wall,

$$W_p = -\pi \int \text{Re}[\sigma_{zr}u_r^* + \sigma_{z\theta}u_\theta^* + \sigma_{zz}u_z^*]rdr. \quad (9)$$

Here, $\mathbf{u} = [u_r \ u_\theta \ u_z]$, and $*$ denotes complex conjugate. The ratio of sound power, then gives the relative distribution in energy between the pipe and the fluid, so that $W = W_0/W_p$. In the analysis that follows, the eigenproblem is solved using a finite element mesh with 10 elements in the fluid, 10 elements in the pipe, and 100 elements in a PML that is attached directly to the outer pipe wall. This takes approximately 2 seconds to obtain and sort the eigenmodes for each frequency using a desktop computer with 8 GB RAM and a 3.2 GHz processor.

3 RESULTS AND DISCUSSION

In this section, predictions obtained using the SAFE-PML model described in the previous section are presented for two example problems. The properties of pipes A and B are listed in Table 1, and here soil is chosen as the surrounding medium. The properties of pipes A and B are chosen to follow those analysed recently by Brennan et al. (Brennan 2017), as this facilitates validation of the numerical predictions before then investigating changes in parameters.

Table 1: Properties of example systems for pipes A and B.

Parameter	Pipe A (Soil)	Pipe B (Soil)	Pipe A (Concrete)
Fluid Density ρ (kg/m ³)	1000	1000	1000
Fluid speed of sound c_0 (m/s)	1500	1500	1500
Pipe Internal Radius, a_0 (mm)	34.1	79.0	34.1
Pipe wall thickness, t (mm)	3.4	11	3.4
Pipe Density, ρ (kg/m ³)	900	900	900
Pipe: Young's Modulus, E (GPa)	2(1+0.06i)	2(1+0.06i)	2(1+0.06i)
Pipe: Poisson's ratio, ν	0.3	0.3	0.3
Surround: Density, ρ (kg/m ³)	2000	2000	2300
Surround: Shear modulus μ (MN/m ²)	241(1+0.15i)	20	1600
Surround: Bulk modulus, B (GN/m ²)	4.5	0.053	19.6671

In Figs. 1 to 4, the real part of the wavenumber and the attenuation for pipes A and B are shown for the $s = 1$ mode. Direct comparison with Brennan et al. (Brennan 2017) may be obtained through the centre values on each plot, and these agree very well with those in the reference article computed using COMSOL. Moreover, additional comparisons that are not shown here also indicate that, as one would expect, very good agreement may be achieved between the SAFE-PML model and a two dimensional COMSOL model, provided sufficiently large PML layers are used in each approach.

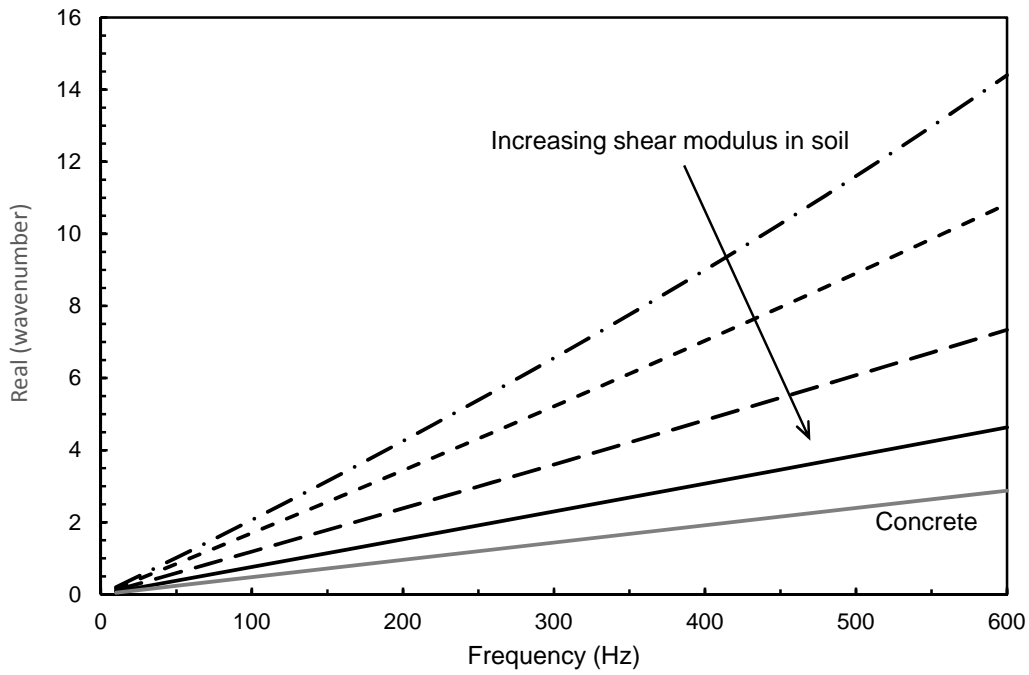


Figure 1: Effect of changing the shear modulus (MN/m^2) on the real part of the axial wavenumber for pipe A.
 \dashdot , $\lambda = 1$; $---$, $\lambda = 50$; $- - -$, $\lambda_{\text{soil}} = 241$; $—$, $\lambda = 1000$; $—$ (grey), $\lambda_{\text{concrete}} = 9000$.

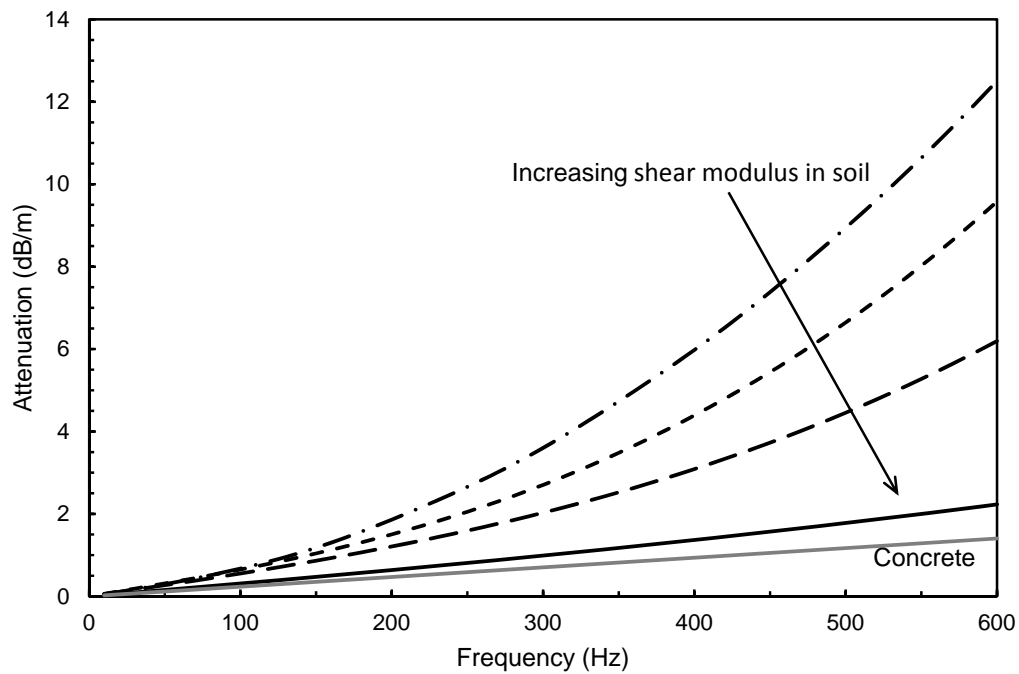


Figure 2: Effect of changing the shear modulus (MN/m^2) on the axial attenuation for pipe A.
 \dashdot , $\lambda = 1$; $---$, $\lambda = 50$; $- - -$, $\lambda_{\text{soil}} = 241$; $—$, $\lambda = 1000$; $—$ (grey), $\lambda_{\text{concrete}} = 9000$.

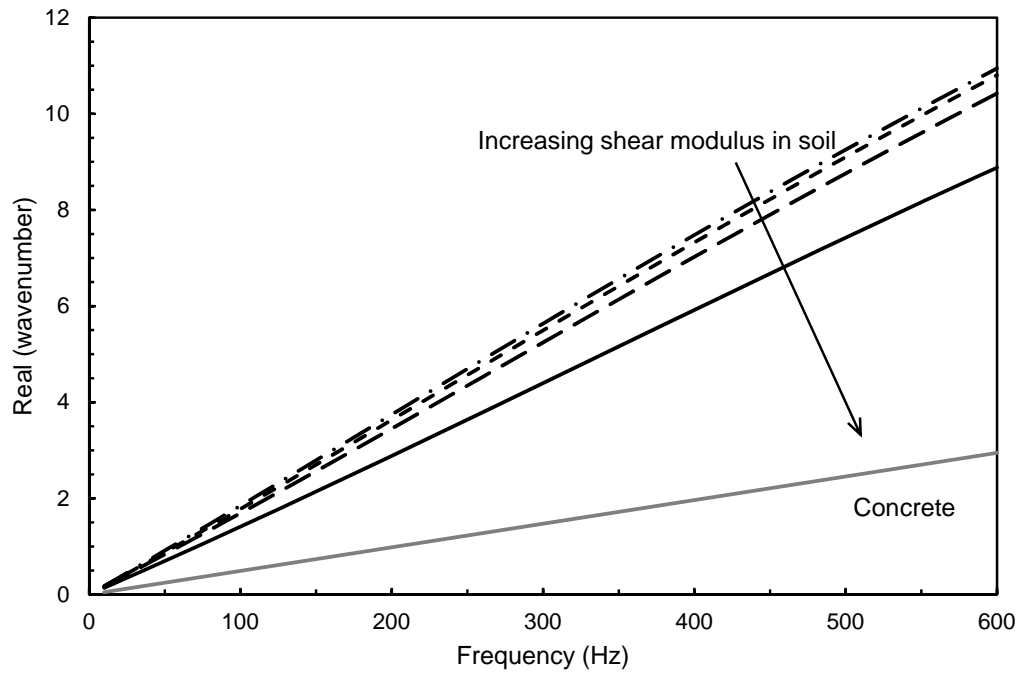


Figure 3: Effect of changing the shear modulus (MN/m^2) on the real part of the axial wavenumber for pipe B.
 - · - ·, $\lambda = 0.1$; - - -, $\lambda = 5$; - - -, $\lambda_{\text{soil}} = 20$; —, $\lambda = 100$; —, $\lambda_{\text{concrete}} = 9000$.

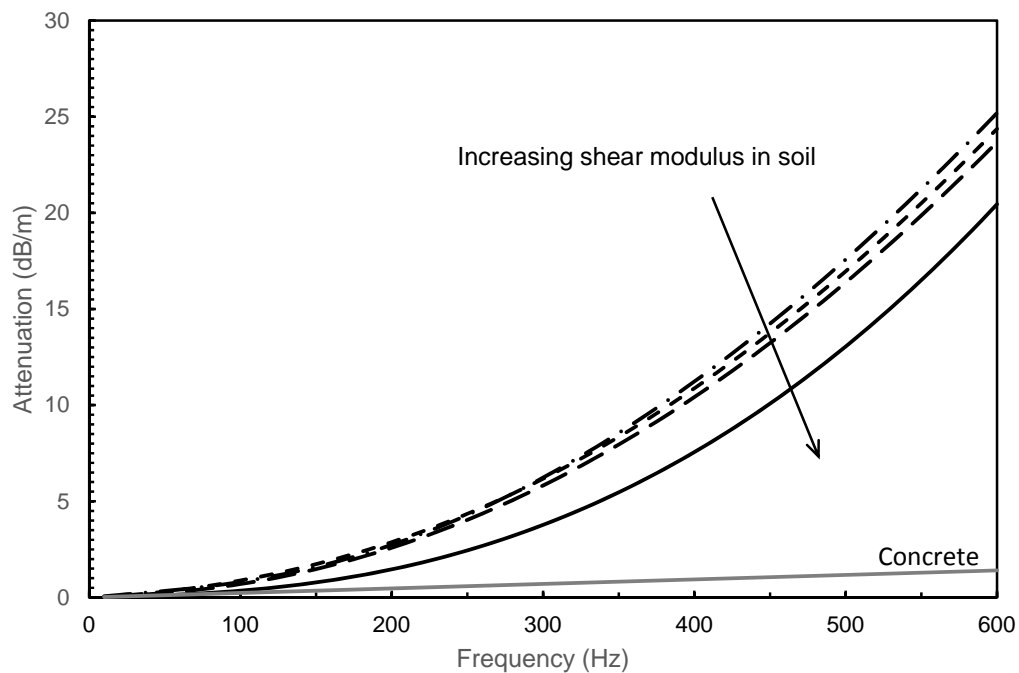


Figure 4: Effect of changing the shear modulus (MN/m^2) on the axial attenuation for pipe B.
 - · - ·, $\lambda = 0.1$; - - -, $\lambda = 5$; - - -, $\lambda_{\text{soil}} = 20$; —, $\lambda = 100$; —, $\lambda_{\text{concrete}} = 9000$.

Figures 1 – 4 also include calculations for different values of the shear modulus, and here it is seen that as the shear modulus is increased the wavenumber and attenuation drops. This is most obvious in the extreme case of substituting concrete as the external material, and here the real part of the wavenumber drops so that the phase speed (roughly equal to 1305.9 m/s over the frequency range shown) begins to approach that of the speed of sound in water (1500 m/s). This is because the increase in shear wave speed in the concrete is higher than in the pipe so that the energy in the pipe is now trapped and cannot escape into the surroundings. This means that when concrete is present the attenuation experienced by the $s = 1$ mode appears because of the losses in the pipe itself, which are included here in the form a loss factor that makes Young's modulus complex. The limiting cases in Figs. 1-4 also illustrate that high values of the shear stiffness in the surrounding medium tend to lower the attenuation of the $s = 1$ mode by limiting energy radiation into the surrounding medium. This effect is consistent in both pipes A and B, and one can also see that as the shear modulus is reduced the attenuation begins to rise when the frequency is increased. This is evidence of greater coupling between the pipe and the surrounding material so that in Figs. 3 and 4 the relatively low values of shear modulus lead to significantly higher levels of attenuation. Therefore, for lower values of shear modulus, the outer displacement of the pipe walls increases for the $s = 1$ mode and so the pipe couples more strongly to the outer material and this will generate acoustic energy that radiates away from the pipe and which can be picked up at the surface.

It is interesting to compare the behaviour observed for the fluid type mode $s = 1$ with the structural type mode $s = 2$ over the low frequency range. This is illustrated for modal attenuation in Fig. 5, where a similar set of limiting cases for the shear modulus are also included. It can be seen in Fig. 5 that the $s = 2$ mode undergoes much higher levels of axial attenuation than the $s = 1$ mode. This is especially true for higher values of shear modulus, where the axial attenuation for concrete is over 200 dB/m. Accordingly, these very high levels of axial attenuation indicate that this mode is unlikely to be detected in testing methodologies that seek to measure the axial propagation of the $s = 2$ mode. Furthermore, it is known to be difficult to excite this particular compressional mode, at least this has been the case for studies in the ultrasonic frequency range [where this mode is known as $L(0,1)$], and so one can expect leaks and ruptures to preferentially excite the $s = 1$, and for the $s = 2$ mode to remain undetected.

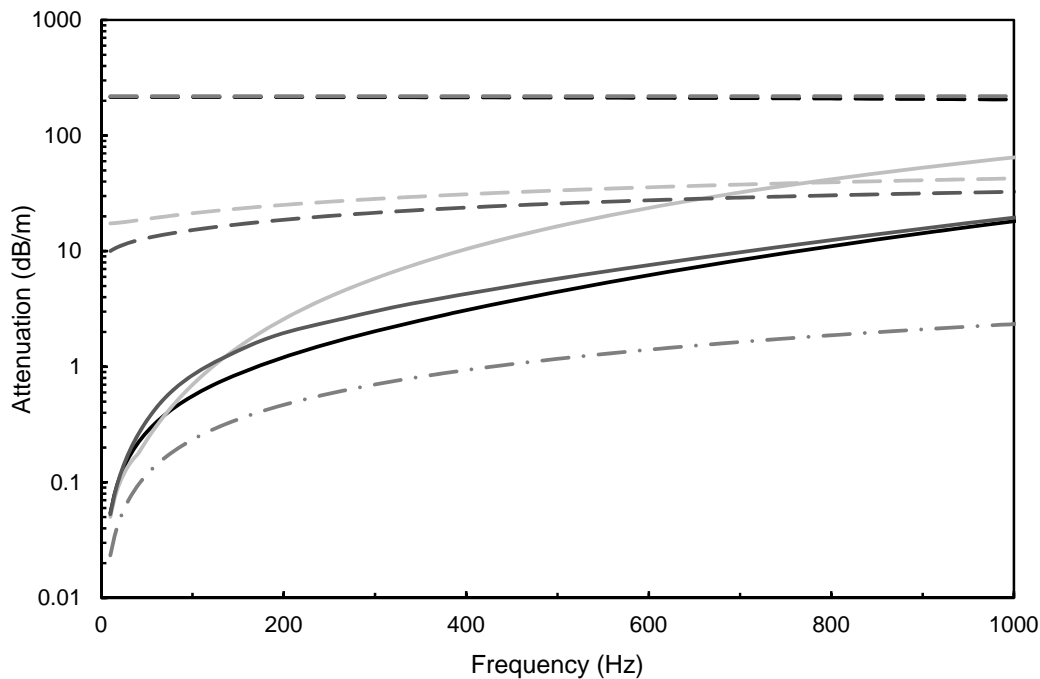


Figure 5: Axial attenuation: Solid line $s = 1$, dashed line $s = 2$.
 —, Pipe A, $\lambda = 241\text{MN/m}^2$; — — —, Pipe B, $\lambda = 20\text{MN/m}^2$;
 — · —, Pipe A, $\lambda = 1\text{MN/m}^2$; · · · ·, Pipe A, $\lambda = 9000\text{MN/m}^2$ (concrete).

In the previous discussion, the importance of energy distribution was introduced, and so in Fig. 6 the relative distribution of sound power between the fluid and the pipe wall is analysed, where W is the ratio of the energy in the fluid divided by the energy in the pipe wall [see Eqs. (8) and (9)]. Note that the relative distribution of sound power is shown here only for the fluid and the pipe wall because it is inappropriate to compute sound power in the surrounding material where a PML is used, as this region uses numerical means to artificially damp down the energy in the outer layer.

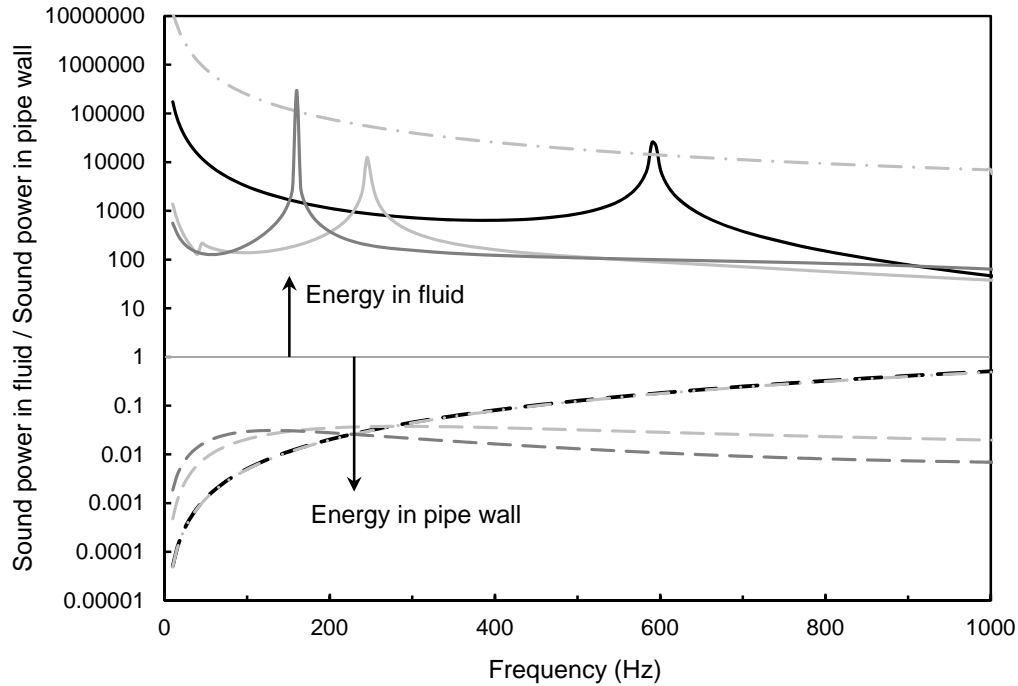


Figure 6: Distribution of energy between the fluid and the pipe wall: Solid line $s = 1$, dashed line $s = 2$.
 ———, Pipe A, $\lambda = 241\text{MN/m}^2$; ———, Pipe B, $\lambda = 20\text{MN/m}^2$;
 - - - - , Pipe A, $\lambda = 1\text{MN/m}^2$; - · - · , Pipe A, $\lambda = 9000\text{MN/m}^2$ (concrete).

In Fig. 6 the differences between the fluid ($s = 1$) and structural ($s = 2$) modes can clearly be seen. Up to a frequency of 1 kHz the energy in the $s = 1$ mode is located primarily in the fluid, whereas the opposite is true for the $s = 2$ mode. However, it should be remembered that when the frequency is increased above 1 kHz the location of energy may change, so that the energy in the fluid mode transfers into the pipe wall, and vice versa. This is why it is important to limit the current experimental methodologies for detecting leaks and ruptures to lower audio frequencies so that energy in the $s = 1$ remains predominantly in the fluid. Furthermore, if the outer region is concrete then it can be seen that the energy is largely trapped in the fluid and, as noted previously, the attenuation drops almost to zero. When concrete is replaced by soil, and the shear modulus drops, the levels of energy in the fluid also begin to drop, although it is seen that for all the examples studied here the energy for the $s = 1$ mode remains predominantly in the fluid. However, there is still energy present in the pipe wall and this can radiate into the surrounding medium and be picked up at the ground surface, although Fig. 6 suggests that this is more likely to happen for lower values of shear modulus.

In Fig. 6 it is interesting also to note the peaks in the energy curves that occur for the $s = 1$ mode, and these are seen to be present for each example. These peaks represent a sudden concentration of energy in the fluid and it may be the case that over these narrow frequency bands the energy available to leak out from the pipe into the surrounding material suddenly drops. The reasons behind this type of behaviour have yet to be identified, however Fig. 6 does illustrate that the propagation of energy in this coupled system is complex, and that small changes in materials properties and/or frequency have the potential to deliver significant changes in the response of the system. The behaviour observed in Figs. 5 and 6 can be further explored by analysing the modes shapes obtained from the numerical simulations. Accordingly, in Fig. 7 the normalised radial displacement is shown at a frequency of 400 Hz, and in Fig. 8 the normalised distribution of pressure (fluid) and shear stress (σ_{rr}) is shown, also at 400 Hz.

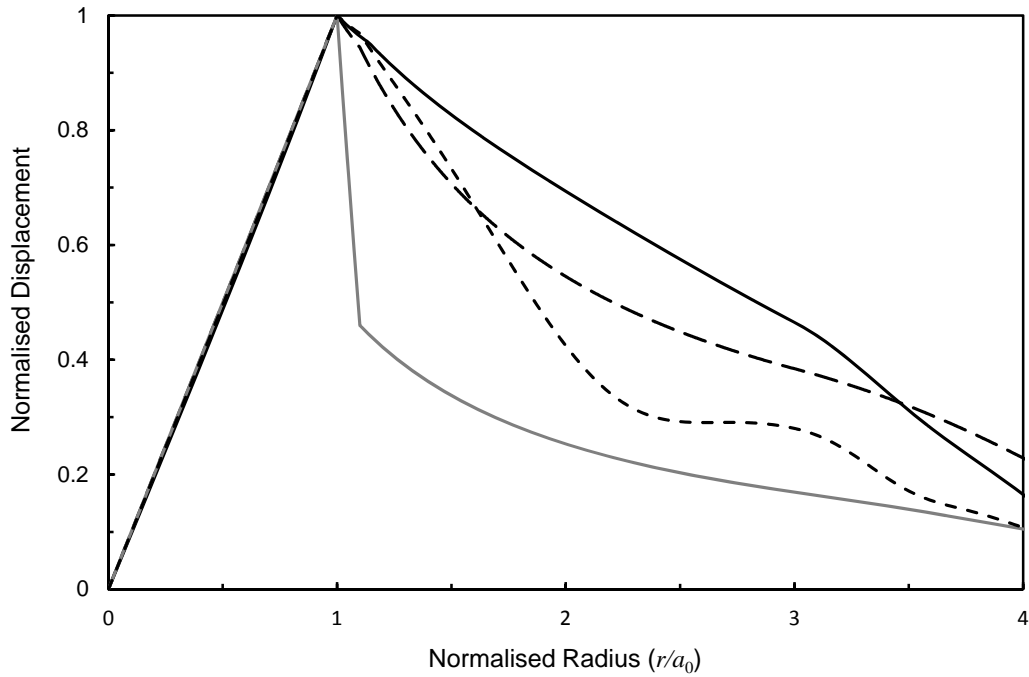


Figure 7: Modal displacement in the radial direction for $s = 1$ at 400 Hz. — — —, Pipe A, $\lambda = 241\text{MN/m}^2$; ———, Pipe B, $\lambda = 20\text{MN/m}^2$; - - - -, Pipe A, $\lambda = 1\text{MN/m}^2$; ———, Pipe A, $\lambda = 9000\text{MN/m}^2$ (concrete).

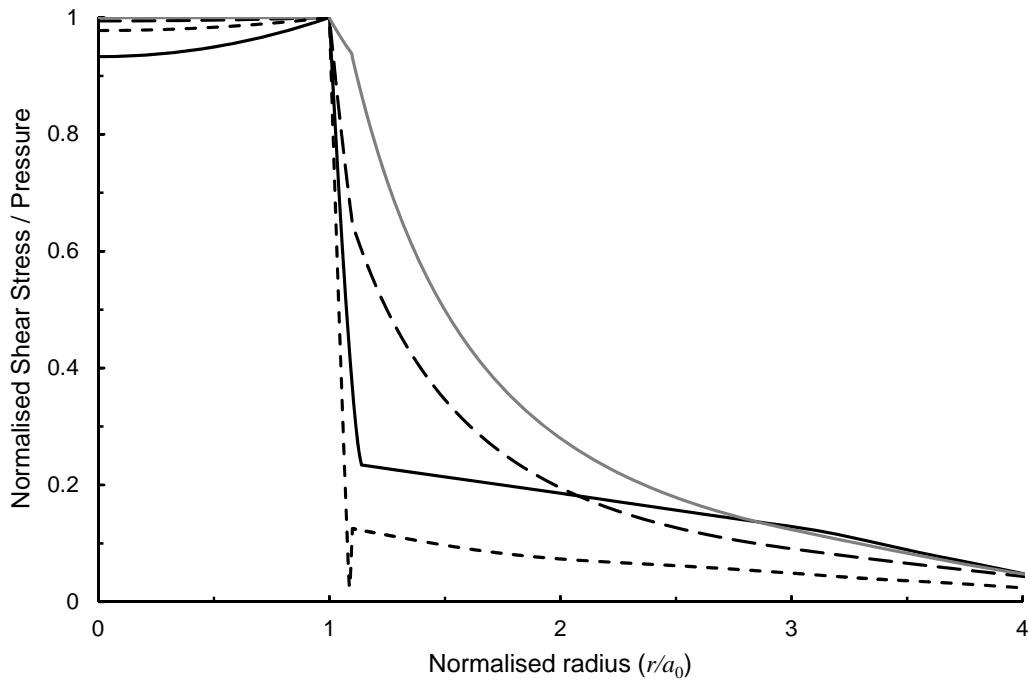


Figure 8: Modal pressure and shear stress (σ_{rr}) distribution for $s = 1$ at 400 Hz. — — —, Pipe A, $\lambda = 241\text{MN/m}^2$; ———, Pipe B, $\lambda = 20\text{MN/m}^2$; - - - -, Pipe A, $\lambda = 1\text{MN/m}^2$; ———, Pipe A, $\lambda = 9000\text{MN/m}^2$ (concrete).

It can be seen in Figs. 7 and 8 that the modal patterns are rather complex, and for this reason the other displacement and shear stresses have been omitted for clarity. Moreover, to compare different examples of pipe geometry, these plots have been normalised against the internal pipe radius. Nevertheless, in Fig. 7 it is seen that, as expected, a very high shear modulus delivers a correspondingly low radial displacement in the surrounding material, although as the shear modulus is reduced these differences are less obvious. This trend tends to be reversed for the shear stress in Fig. 8, and here the fluid pressure in the pipe is seen to be almost constant over this frequency range. A planar sound pressure distribution is consistent with energy being located predominantly in the fluid, and here it is not surprising to see that when concrete surrounds the pipe the fluid pressure is almost constant.

4 CONCLUSIONS

The propagation of acoustic energy in water-filled buried pipes is complex and very sensitive to the relative values of the different parameters that make up the coupled system. At low frequencies, acoustic energy is seen largely to be concentrated in the fluid for the $s = 1$ mode. Moreover, it is difficult to excite the $s = 2$ mode and, even if this was possible, this mode is likely to experience high levels of axial attenuation over this low frequency range. For this reason, the $s = 1$ mode is the one used to detect leaks and ruptures in water-filled buried pipes at low frequencies. However, it is seen that whilst this approach is likely to work well when one is attempting to detect axial wave propagation, the problem becomes more complex when detecting energy radiating to the ground surface above a buried pipeline. For example, high values for the shear modulus in the surrounding material, such as that associated with concrete, suppresses radial wall motion in the pipe so that the energy remains largely trapped within the fluid. For lower values of shear modulus, such as those associated with soil, then the energy is still predominantly located in the fluid. However the displacement of the outer wall is sufficient to enable energy to leak out from the pipe and this can be picked up at the ground surface, although the levels of energy radiating will depend on the relative properties of the pipe/soil interface, and it also appears to be possible that over narrow frequency bands energy may suddenly concentrate in the fluid. This means that the levels of energy radiating outwards from the pipe are likely to be very sensitive to relative material properties and small changes in frequency. This suggests that it is likely to be difficult to obtain very good quantitative agreement between theoretical predictions and experimental measurements and ground surface vibrations, especially if one also accounts for the likely inhomogeneities in a surrounding material such as soil or sand, and the effects of porosity (which have not been included here). Accordingly, a qualitative investigation of expected behaviour, such as the one conducted here, is likely to remain useful when helping to guide future experimental understanding and to improving the ability to locate leaks and ruptures at the ground surface.

ACKNOWLEDGEMENTS

Michael Brennan would like to acknowledge the financial support from FAPESP, Process Nos. 2013/50412-3 and 2015/50312-4.

REFERENCES

- Brennan, M.J., Karimi, M., Almeida, F.C.L., Kroll de Lima, F., Ayala, P.C., Obata, D., Paschoalini, A.T., Kessissoglou, N. 2017. 'On the role of vibro-acoustics in leak detection for plastic water distribution pipes'. International Conference on Structural Dynamics, EURO-DYN 2017, In Press.
- Duan, W., Kirby, R., Mudge, P., Gan, T-H. 2016. 'A one dimensional numerical approach for computing the eigenmodes of elastic waves in buried pipelines'. *Journal of Sound and Vibration* 384: 177-193.
- Gao, Y., Sui, F., Muggleton, J.M., Yang, J. 2016. 'Simplified dispersion relationships for fluid-dominated axisymmetric wave motion in buried fluid-filled pipes'. *Journal of Sound and Vibration* 375: 386-402.
- Gao, Y., Muggleton, J.M., Liu, Y., Rustighi, E. 'An analytical model of ground surface vibration due to axisymmetric wave motion in buried fluid-filled pipes'. *Journal of Sound and Vibration* 395: 142-159.
- Leinov, E., Lowe, M.J.S., Cawley, P. 2015. 'Investigation of guided wave propagation and attenuation in pipe buried in sand'. *Journal of Sound and Vibration* 347: 96-114.
- Muggleton, J.M., Brennan, M.J., Pinnington, P.J. 2002. 'Wavenumber prediction of waves in buried pipes for water leak detection'. *Journal of Sound and Vibration* 249: 939-954.
- Muggleton, J.M., Yan, J. 2013. 'Wavenumber prediction and measurement of axisymmetric waves in buried fluid-filled pipes: inclusion of shear coupling at a lubricated pipe/soil interface'. *Journal of Sound and Vibration* 332: 1216-1230.
- Nilsson, C.-M., Finnveden, S. 2008. 'Waves in thin-walled fluid-filled ducts with arbitrary cross-sections'. *Journal of Sound and Vibration* 310: 58-76.